Water Supply

Water Supply Vol 24 No 3, 847 doi: 10.2166/ws.2024.034

Improving the performance of a condensation water production system through support vector machine modeling and genetic algorithm optimization

Shayan Hajinajaf[a], Shaban Ghavami Jolandan[a,*], Hassan Masoudi[a] and Abbas Rohani[b]

[a] Department of Biosystems Engineering, Faculty of Agriculture, Shahid Chamran University of Ahvaz, Ahvaz, Iran
[b] Department of Biosystems Engineering, Faculty of Agriculture, Ferdowsi University of Mashhad, Mashhad, Iran
*Corresponding author. E-mail: s.ghavami@scu.ac.ir

AR, 0000-0002-4494-7058

ABSTRACT

Water scarcity is recognized as a critical global concern and one viable solution involves extracting water from atmospheric humidity by leveraging subterranean coldness. This study meticulously evaluates the operational efficacy of a water production system by examining four pivotal factors: buried pipe length (TL), air flow rate (AFR), air temperature (AT), and air humidity (AH). A positive correlation between these variables and water vapor production is established, with AT exerting the most pronounced influence. Significantly, the analysis of variance reveals the main and interactive effects of the variables, except for TL × AFR, at a 5% significance level. To enhance understanding of the intricate interplay among these factors, a proficient least squares support vector machines model is devised, employing a radial basis function kernel. This model demonstrates an impressive 98% concurrence between projected and empirical data, with a minimal error of 0.66 mL and 5.99%. An in-depth sensitivity analysis underscores the differential impact of AT, AH, TL, and AFR on water vapor (WV) prediction. Optimal values of 3.98 m, 6.89 m^3/h, 46.30 °C, and 86.62% for TL, AFR, AT, and AH, respectively, are obtained through subsequent optimization of independent variables using genetic algorithms, resulting in a notable water production of 23.61 mL.

Key words: condensation, genetic algorithm, support vector machine, water production system

HIGHLIGHTS

- Air humidity can address rural water scarcity.
- Air temperature, humidity, flow rate, and pipe length affect water volume production.
- The support vector machine model with radial basis function kernel is the best solution for predicting water volume.
- The least squares support vector machines model shows a 98% agreement between predicted and experimental data.
- Genetic algorithms resulted in optimized independent variable values and 23.61 mL water production.

GRAPHICAL ABSTRACT

NOMENCLATURE

AFR	Air flow rate
AH	Air humidity
AT	Air temperature
GA	Genetic algorithm
AWH	Atmospheric water harvesting
TL	Buried pipe length
WPS	Water production system
WV	Water volume
R^2	Coefficient of determination
RBF	Radial basis function
MAPE	Mean absolute percentage error
RMSE	Root mean square error
SVM	Support vector machine

1. INTRODUCTION

The escalating challenge of global freshwater scarcity underscores the crucial need for innovative solutions in water management. With only 2.5% of the Earth's surface covered by water, it plays a vital role in essential activities such as drinking, agriculture, and industrial processes. This scarcity gains more significance in light of the projected population surge to 9.7 billion by 2050, accompanied by the rapid escalation of water consumption that surpasses population growth rates (Tzanakakis *et al.* 2020). Moreover, the situation is further exacerbated by the impacts of climate change, global warming, and contamination. Relying solely on precipitation as a viable freshwater source becomes unfeasible due to contamination risks. In response to these challenges, innovative approaches, such as rainwater harvesting and fog water collection, have been explored in regions characterized by high humidity levels (Bergmair 2015). However, large-scale desalination projects

have remained economically viable primarily near water sources, resulting in escalated costs for remote regions. Consequently, the quest for alternative freshwater sources has become imperative, with atmospheric water, estimated at a substantial volume of approximately 13 trillion m^3, emerging as a promising and viable solution (Gerard & Worzel 1967). The quantity of water harvested from the atmosphere relies on atmospheric and geographical conditions, alongside the design of the water absorption system (Hassan *et al.* 2023). This study delves into the untapped potential of utilizing atmospheric water resources through a specifically designed condensation water production system (WPS). By leveraging advanced machine learning (ML) techniques, the system's operational efficiency and water extraction output are significantly enhanced. Notably, the dehumidifier's size and structure play a crucial role in determining the volume of extracted water, highlighting the importance of optimization and tailoring the system to maximize its performance.

Recent years have witnessed substantial advancements in the realm of atmospheric water harvesting (AWH), with a notable emphasis on enhancing the efficiency and efficacy of water collection. Extensive research and experimentation have been undertaken to investigate diverse methodologies and materials for this objective. Various materials fulfilling distinct functions have been employed in WPSs utilizing air-cooled adsorption-based methods. For example, the collection of 7.7 kg of water per cycle is enabled by the integration of an activated carbon fiber felt with a silica solution – LiCl30 (Wang *et al.* 2021). In an alternative system, 159 g of water per cycle is efficiently harvested by a silica gel model (Sleiti *et al.* 2021). Furthermore, superior rates of water harvesting are achieved by a dual-stage system employing zeolite material and solar energy (LaPotin *et al.* 2021). Researchers conducted a review on surfaces with modified morphology and wettability for water harvesting in desertification areas. The exploration of alternatives becomes necessary due to the high water transport costs in desertification regions. Meeting plant water requirements through freshwater produced via dewing can achieve a reduction in irrigation costs. The technologies discussed in the review focus on preparing water harvesting materials with modified microstructure and wettability. Common morphologies include surfaces with a bump array and counter wettability. Although dew productivity in desert areas may be less efficient than in experiments, the promise for dew water production is shown by a hydrophobic surface with a submicron-scale hydrophilic spherical cavity array (Zhang *et al.* 2023a). A groundbreaking study was conducted on water harvesting from fog and dew in semi-arid and arid regions of Syria, addressing water scarcity exacerbated by climate change and the consequences of war. The experimental results indicate promising potential for dew and fog water harvesting as a supplementary freshwater source in Syria, offering renewable and relatively clean alternatives amid water scarcity challenges (Khalil *et al.* 2022). An innovative approach for air humidification and water production involves a multi-stage desiccant wheel system integrated with a heat pump. Through the utilization of a vapor compression cycle, the system efficiently condenses humid air, resulting in a significant water production rate of 32.5 kg/h (Tu & Hwang 2019). A quasi-continuous system, driven by solar energy and utilizing a microporous aluminum-based metal-organic framework (MOF), achieved significant water production rates. Indoor experiments demonstrated a water production of approximately 1.3 L/kg of adsorbent per day. In the Mojave Desert, the system yielded 0.7 L/kg of adsorbent (Hanikel *et al.* 2019). In the context of Saudi Arabia, various devices for extracting water vapor from air were developed and examined. One such example involved the utilization of a trapezoidal prism filled with a black cotton rag soaked in calcium chloride, resulting in a water yield of 1.06 L/m^2 per day (Elashmawy & Alatawi 2020). The literature review explores two primary methods for AWH: active cooling and dew water harvesting. Active cooling methods, which require electrical power, exhibit a high water yield when operated continuously. In contrast, dew water harvesting is unaffected by climatic conditions and can supply water to environmentally sensitive areas (Shafeian *et al.* 2022). A typical yield of 2–4.2 L/kWh is typically achieved by commercial active water harvesting devices (Tashtoush & Alshoubaki 2023). Based on climatic data, efficiency in hot, low-humidity regions is demonstrated by air-cooling systems, while desiccant systems are recommended for cold, low-humidity areas. Both preferable technologies include active air-cooling, which exhibits greater effectiveness in humid areas (40–60% relative humidity) and temperatures ranging from 0 to 20 °C (Peeters *et al.* 2021). The literature review highlights various techniques for harvesting atmospheric water vapor, with particular attention to the prevalence of surface cooling and desiccant methods. Adsorbent-based approaches are currently emphasized in research due to their inherent advantages (Wahlgren 2001). Nevertheless, a significant amount of energy is consumed by surface cooling, whereas the potential to harvest 7.9 L of water per day with reduced energy consumption is demonstrated by a vapor compression refrigeration device. Despite the theoretical proposal for a solar system utilizing concentrated photovoltaic thermal units and Stirling engines, energy consumption remains relatively high. According to a computer model based on a vapor compression cycle, the estimated energy consumption is 220–300 Wh/L to produce 22–26 L of water daily. Furthermore, the ability to operate under various weather conditions is

showcased by an atmospheric water-gathering device employing a vapor compression cycle (Talib *et al.* 2019). Compact and efficient cooling and heating devices that utilize the Peltier effect to generate cooling through an electric current are Peltier devices (Tu & Hwang 2020). Various applications of Peltier devices for capturing atmospheric water have been examined in research, including the development of a solar-powered device for irrigation and remote regions. Different methods and designs involving Peltier devices for AWH with solar energy have been analyzed, covering water production efficiency, agricultural applications, and integration with solar distillers (Koc *et al.* 2020). Water harvesting devices based on Peltier devices rely on the temperature differential between materials to generate an electric current, facilitating cooling below the dew point and the subsequent condensation of moisture (Kadhim *et al.* 2020). The evaluation of fog water harvesting for supplementary irrigation in rain-fed winter wheat in Ardabil, Iran, involved the measurement of daily water collection during foggy periods in 2021 using a standard fog collector. The study aimed to address water scarcity in arid regions. With 30 and 60 mm of water collected, irrigation was applied, covering 26 and 34% of the water deficiency, leading to yield increases of 0.6 and 1.7 tons/ha, respectively (Kanooni & Kohan 2023).

The field of AWH has witnessed a surge of interest in leveraging ML techniques to both simulate and optimize WPS parameters. A recent study exemplified this trend by utilizing ML for the computational screening of MOFs with superior water capture capabilities. Through the analysis of a vast dataset comprising over 6,013 experimental and 137,953 hypothetical MOFs, the study convincingly demonstrated the critical role of heat adsorption (Qst) in the process of extracting water from atmospheric N_2 and O_2. Employing a range of algorithms – including random forest (RF), gradient boosted regression trees, and neighbor component analysis (NCA) – researchers efficiently elucidated the intricate interplay between six key chemical descriptors and water capture performance. Notably, the highly accurate NCA model pinpointed the dominant influence of Qst, achieving an impressive coefficient of determination (R^2) value of 0.97 for CoRE-MOFs. Furthermore, the model successfully predicted the selectivity of hypothetical MOFs with an R^2 of 0.86, highlighting its potential for guiding the design of next-generation water harvesting materials (Li *et al.* 2022). This study centers on the innovative incorporation of a novel desiccant mechanism, utilizing highly hygroscopic silica gel within a double-slope half-cylindrical basin solar still for the efficient extraction of water from ambient air. Furthermore, a Neuro-fuzzy Inference System (ANFIS) model is successfully implemented to predict system productivity under diverse ambient temperatures and solar irradiance conditions. This model demonstrates a remarkable concordance with the experimental findings, highlighting its potential as a valuable tool for optimizing the water production process (Essa *et al.* 2020). The significance of an ML approach for predicting water adsorption in MOFs is emphasized in another study, aiding in the identification of optimal MOFs for effective water harvesting. Incorporating structural and chemical features, along with operational conditions as crucial descriptors, a high degree of accuracy in forecasting water adsorption properties is exhibited by the ML models (Zhang *et al.* 2023b).

The optimization of the extreme learning machine (ELM) model for estimating daily reference evapotranspiration (ETo) in China's Hetao irrigation district (HID) was carried out. Superior accuracy compared to other algorithms and empirical models was demonstrated by the Gray Wolf Optimization-ELM (GWO-ELM) model, which incorporated key input variables and utilized the Gray Wolf Optimizer. This model, particularly with the mass transfer combination, is recommended for precise daily ETo estimation in HID (He *et al.* 2022). An investigation into predicting evapotranspiration (ET) in various agro-climatic regions of India was conducted using an artificial neural network (ANN) model coupled with principal component analysis (PCA). The challenges encountered by the Penman–Monteith ET model in Indian stations were addressed by employing sensitivity analysis to identify key variables. Through the application of PCA, an ANN model was developed, yielding promising results. A 98% variability explanation in ET0 was achieved, and high accuracy was demonstrated compared to the Penman–Monteith ET estimate (Abraham & Mohan 2023). Diverse soft computing approaches for soil moisture (SM) estimation were assessed by Moazenzadeh *et al.* (2022). The evaluation involved classical ANFIS and its hybrids with bio-inspired metaheuristic optimization methods. By utilizing Istanbul Bolge station data, the study demonstrated that SM estimates were significantly enhanced by hybrid models. Among them, ANFIS-WOA (Whale Optimization Algorithm) exhibited the lowest errors across various SM intervals (Moazenzadeh *et al.* 2022). Some researchers conducted a comparison of the integration of neural network and fuzzy logic decision-making with a bilayered neural network for simulating daily dew point temperature (DPT). The results demonstrate a strong agreement between the ANFIS method and observed data, indicating promise for predicting DPT at different locations. The stability of the ANFIS model across different numbers of membership functions was revealed through a comprehensive comparison with the bilayered neural network (Zhang *et al.* 2022). In another study, the feasibility of predicting monthly

pan-evaporation (EP) with limited climatic input data, specifically focusing on temperature, was investigated using a relevance vector machine tuned with improved manta ray foraging optimization (RVM-IMRFO). A comparison was conducted to assess the accuracy of RVM-IMRFO against other optimization-tuned RVM models, namely, GWO, WOA, and Manta Ray foraging optimization. Superior performance in terms of overall mean values of root mean square error (RMSE) and R^2 was observed for RVM-IMRFO, highlighting its effectiveness compared to the other models (Adnan *et al.* 2023). A study on precise air temperature (AT) forecasting, a crucial meteorological parameter for environmental quality management in the world's warmest and coldest regions, was conducted by another group of researchers. A hybrid intelligent model was utilized, combining an ANN with the heuristic Honey Badger Algorithm (HBA-ANN). Comparisons with classical ANN and gene expression programming models using statistical criteria, Taylor and scatter diagrams, revealed that the HBA-ANN model outperformed in both the training and testing phases (Zhou *et al.* 2023). A study was conducted to estimate daily EP in various agro-climatic zones (ACZ) using a hybrid support vector regression (SVR) model optimized with the Salp Swarm Algorithm (SVR-SSA), alongside the gamma test. The hybrid SVR-SSA model was found to be more suitable, robust, and reliable for daily EP estimation in diverse ACZs (Malik *et al.* 2021). An investigation was conducted to predict the durability of high-performance concrete in challenging cold and marine environments, with a specific focus on resistance to chloride ion penetration. An integrated prediction model that combined the RF and least squares support vector machine (LS-SVM) algorithms was introduced by the researchers. The results demonstrated that the RF-LS-SVM hybrid approach effectively predicted concrete resistance to chloride penetration with superior accuracy compared to typical ML algorithms (Liu *et al.* 2022). The study focused on the evaluation and forecasting of stability in smart grid systems. Recognizing the growing demand for accurate stability predictions resulting from increased integration of green energy and infrastructure development, a novel approach was introduced. The multi-layer perceptron-ELM (MLP-ELM) technique and PCA were employed for feature extraction in this approach. Simulation results underscored the superiority of the MLP-ELM approach over traditional techniques, achieving high accuracy (Alsirhani *et al.* 2023). The challenge of predicting the water quality index in rivers, crucial for effective pollution prevention, was addressed. Acknowledging the nonsmooth and nonlinear nature of water quality data and the complex interrelationships among parameters, a novel hybrid model was proposed: the Back Propagation Neural Network (BPNN) combined with the Adaptive Evolutionary Artificial Bee Colony (AEABC) algorithm. The superior performance of the AEABC-BPNN model over other algorithms, exhibiting a lower mean square error (MSE), was showcased through the experimental result (Chen *et al.* 2023). An innovative hybrid model for water quality prediction was introduced by Wang *et al.* (2023), aiming to overcome challenges posed by the nonlinearity, instability, and randomness of water quality parameters. The model integrated variational mode decomposition (VMD) and an improved grasshopper optimization algorithm (IGOA) to optimize the long short-term memory neural network (LSTM). The IGOA-LSTM model outperformed existing models, showcasing superior accuracy in short-term water quality prediction (Wang *et al.* 2023). An ensemble deep learning model was proposed by the researchers, which efficiently decomposes runoff series using VMD and extracts features with a convolutional neural network. When evaluated with daily runoff data from the Wei River Basin, the model outperformed other models, demonstrating lower RMSE and superior peak flood prediction capability (Wu *et al.* 2023).

Addressing the pressing issue of global water scarcity, particularly in resource-constrained rural communities, this study investigates a novel WPS that extracts water from the air through condensation. Recognizing the potential of this innovative approach, the research meticulously evaluates its performance, employing state-of-the-art techniques to ensure robust and comprehensive assessment. For accurate appraisal, the study leverages the powerful support vector machine (SVM) to meticulously simulate the WPS's capabilities under diverse operating conditions. This rigorous approach is further enhanced by the integration of genetic algorithms (GAs), which optimize the system's input variables – namely, buried pipe length (TL), air flow rate (AFR), AT, and air humidity (AH). By meticulously analyzing the influence of these critical factors, the study identifies optimal settings that significantly enhance the overall efficiency of the WPS. This optimization not only represents a valuable contribution to the existing body of knowledge but also signifies a significant advancement in the field of water harvesting systems. The study's rigorous analysis and targeted optimization pave the way for the development of practical and highly efficient air-to-water systems. By shedding light on the importance of critical variables like TL, AFR, AT, and AH, the research provides valuable insights for the design and implementation of future WPSs. Ultimately, this investigation contributes to the broader understanding of sustainable water management and offers promising solutions to alleviate water scarcity challenges, particularly in vulnerable rural communities.

2. MATERIALS AND METHODS

2.1. Constructing and evaluating a WPS

Motivated by the pressing need for sustainable water solutions, particularly in vulnerable rural communities, this study presents a novel WPS designed to extract water from ambient AH. As depicted in Figure 1, the system comprises two distinct sections: a subterranean network and an above-ground control unit. The subterranean section employs copper pipes, strategically positioned solenoid valves, and a dedicated water collection tank for the harvested condensate. Conversely, the above-ground control unit houses a spacious cubic chamber ($2 \times 2 \times 2$ m^3), electronic control boards, temperature and humidity sensors, air fans, levers controlling the solenoid valves, and environmental conditioning equipment. Specifically, the air circulating within the chamber is meticulously adjusted for temperature and humidity using an air conditioner, a heater, and a humidifier before being directed into the underground pipe network at controlled flow rates regulated by the feeding fan. A more detailed account of the system configuration can be found in the work of Hajinajaf *et al.* (2021).

Several key factors can influence the water production capacity of the system. To thoroughly assess its performance, a comprehensive investigation was undertaken examining the impact of four critical variables on the generated water volume (WV): AT (encompassing a range of 20, 30, 40, and 50 °C), AH (spanning 30, 50, 70, and 90%), AFR (varied across 2.5, 5, and 7.5 m^3/h), and TL (evaluated at both 2 and 4 m). These experiments were conducted within Ahvaz City, Iran (precisely located at 31 °18′17″N 48 °40′42″E). Notably, Ahvaz possesses a subtropical hot desert climate (Köppen classification BWh), characterized by prolonged, scorching summers and brief, mild winters. During summer months, temperatures routinely surpass 45 °C and occasionally exceed 50 °C.

2.2. Experimental design and performance evaluation of a WPS

The efficacy of the WPS was rigorously evaluated through a comprehensive experimental investigation implemented using a completely randomized factorial design. This robust design, with each treatment replicated three times, ensured the reliability

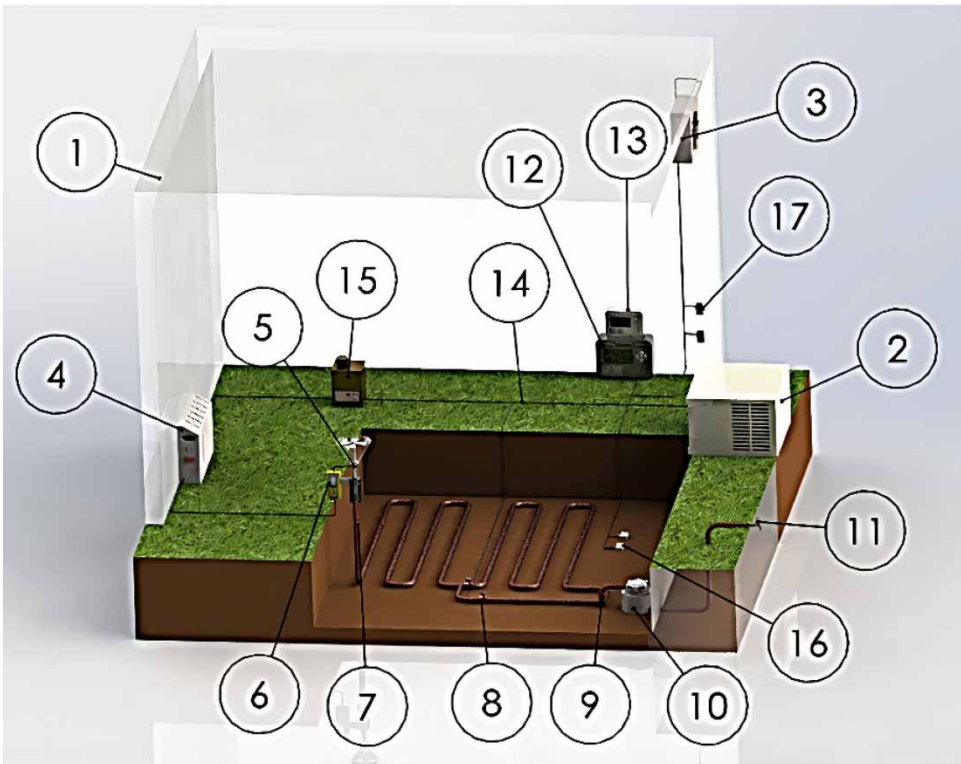

Figure 1 | Components of the studied WPS from AH: (1) chamber, (2) cooler, (3) wall fan, (4) heater, (5) feeding fan, (6) flow meter, (7) copper tubes, (8) electrical valves, (9) water inlet to the tank, (10) tank, (11) water drain valve, (12) and (13) control boards, (14) connecting wires, (15) vaporizer, (16) temperature and humidity sensors (buried), and (17) temperature and humidity sensors.

and validity of the obtained results. The study sought to elucidate the influence of four critical factors on the rate of water production: AT, AH, AFR, and TL. Each factor was evaluated across multiple levels:

- AT: 20, 30, 40, and 50 °C
- AH: 30, 50, 70, and 90%
- AFR: 2.5, 5, and 7.5 m^3/h
- TL: 2 and 4 m

This combination of factors yielded a total of 288 unique experimental tests, providing substantial data for rigorous analysis. To assess the independent variables' influence, an analysis of variance (ANOVA) was conducted using Minitab software. In addition, correlation analysis was employed to explore the potential interrelationships between the variables. The detailed findings from these meticulous analyses will be presented in the subsequent results and discussion sections of this study.

2.3. An SVM for predicting performance in a WPS

To comprehensively explore the relationships between AT, AH, AFR, TL, and WV production in the condensation WPS, an LS-SVM model was selected. Recognized for its adeptness in handling both linear and nonlinear relationships, the LS-SVM presented itself as a fitting tool for undertaking regression analysis. Through the application of LS-SVM, the study aimed to establish a thorough understanding of how these independent variables impact WV production within the system, ultimately enabling the optimization of the production process and enhancement of overall system performance.

During the data preprocessing stage, both the independent (AT, AH, AFR, TL) and dependent (WV) variables were standardized to a mean of 0 and a standard deviation of 1. This standardization technique was implemented to ensure equal weighting of each variable within the LS-SVM model. The model itself was constructed by randomly partitioning the dataset into two distinct subsets: an 80% training set and a 20% testing set. The training set was utilized to train the LS-SVM model, while the testing set served to evaluate its predictive accuracy. This approach permitted a robust assessment of the model's performance and its suitability for analyzing the complex relationships within the WPS.

The LS-SVM model was developed using the following equation:

$$f(x) = \text{sign}(w^T x + b) \tag{1}$$

where the predicted value of WV is represented by $f(x)$, while w denotes the weight vector. In addition, $\varphi(x)$ represents the mapping function used in the model and b is the bias term.

The LS-SVM model has been formulated using the following equation. To capture the nonlinear relationships between the independent variables and water vapor (WV) production, four distinct kernel functions were employed to transform the input variables into higher-dimensional spaces. These kernels encompassed the linear kernel (Equation (2)), polynomial degree 2 (Poly2) kernel (Equation (3)), polynomial degree 3 (Poly3) kernel (Equation (4)), and radial basis function (RBF) kernel (Equation (5)).

$$K(x, x_i) = x^T x_i \tag{2}$$

$$K(x, x_i) = (\gamma(x^T x_i) + r)^2 \tag{3}$$

$$K(x, x_i) = (\gamma(x^T x_i) + r)^3 \tag{4}$$

$$K(x, x_i) = \exp(-\gamma \|x - x_i\|^2) \tag{5}$$

where $K(x, x_i)$ is the kernel function, x and x_i are the input vectors, γ is the kernel parameter, and r is the independent term.

To optimize the LS-SVM model for accurate water volume (WV) prediction, training employed three distinct solver algorithms available within MATLAB: Sequential Minimal Optimization (SMO), Incremental Single Data Algorithm (ISDA), and L1 Regularized Quadratic Programming (L1QP). Each algorithm offers unique advantages in optimizing model parameters for various problems. During training, the algorithm aimed to minimize the MSE between the predicted and actual WV production values. This minimization process, crucial for accurate model fitting, was achieved by concurrently optimizing the model's hyperparameters, namely, the kernel parameter (γ) and the regularization parameter. The optimal values of these parameters were determined through an iterative process that balanced model complexity and generalization ability.

2.4. Maximizing the performance of a WPS using GA

Driven by their effectiveness in tackling complex optimization problems, GAs have found widespread adoption across various fields. Recognizing the system's intricate interplay of factors, this study employed a GA to optimize the design of the WPS and maximize its overall performance. The primary objective was to identify the optimal configuration of design parameters (AT, AH, AFR, and TL) that would yield the highest water production capacity. To achieve this, an objective function based on an SVM model was utilized to guide the optimization process. This function effectively quantified the performance of each candidate solution. The GA operated with a population of potential solutions, each representing a specific combination of design parameters. Through an iterative process of selection, crossover, and mutation, the algorithm generated successive generations of progressively improved solutions. During selection, individuals with higher objective function values were preferentially chosen to contribute their 'genes' to the next generation. The crossover and mutation operations then played a crucial role in introducing diversity into the population, allowing the algorithm to explore broader areas of the design space and avoid premature convergence on suboptimal solutions.

MATLAB's Global Optimization Toolbox provided the platform for implementing the GA algorithm. Careful consideration was given to defining the design parameters, their respective boundaries, and the objective function targeted for optimization. The GA configuration employed a population size of 50 individuals, employing a linear feasible creation function to ensure valid solutions. To effectively guide the selection process, a rank-based scaling function was utilized, prioritizing individuals with superior objective function values. In addition, a 5% elite count ensured that high-performing solutions always contributed their 'genes' to subsequent generations. Further diversification was introduced through an adaptive feasible mutation function, while genetic information exchange was facilitated by a scattered crossover function. The optimization process ran for 500 generations, allowing the algorithm to thoroughly explore the design space and converge upon the optimal solution for maximizing water production.

2.5. Evaluation criteria for assessing the performance of the SVM model

The performance of the SVM model in predicting water volume (WV) production within the condensation WPS was evaluated using three key metrics: the R^2, the RMSE, and the mean absolute percentage error (MAPE). R^2 quantifies the strength of the correlation between predicted and observed values, with higher values indicating greater agreement. RMSE, on the other hand, measures the average magnitude of the discrepancies between predicted and observed values, with lower values signifying better model fit. Finally, MAPE evaluates the average percentage difference between predicted and observed values, providing a relative measure of error. The formulations for these metrics are provided in Equations (6)–(8), respectively. Selection of the optimal SVM model relied on identifying the one exhibiting the highest R^2 and the lowest values for both RMSE and MAPE.

$$R^2 = \frac{\left(\sum_{i=1}^{n}(w_{o.i} - \bar{x}_o)(w_{p.i} - \bar{w}_p)\right)^2}{\sum_{i=1}^{n}(w_{o.i} - \bar{w}_o)^2 \times \sum_{i=1}^{n}(w_{p.i} - \bar{w}_p)^2} \tag{6}$$

$$\text{RMSE} = \sqrt{\frac{\sum_{i=1}^{n}(w_{o.i} - w_{p,i})^2}{n}} \tag{7}$$

$$\text{MAPE} = \frac{1}{n}\sum_{i=1}^{n}\frac{w_{o.i} - w_{p,i}}{w_{o.i}} \times 100 \tag{8}$$

where w_o represents the observed value, w_p represents the predicted value, $\bar{w}_o$ represents the average observed value, and w_p represents the average predicted value.

3. RESULTS AND DISCUSSION

In this section, a thorough analysis was undertaken to assess the significance of each system variable in influencing water production. Expanding upon this groundwork, a robust SVM model was formulated to predict the system's performance. The predictive results derived from the SVM model are subsequently presented and discussed. Finally, by harnessing the

capabilities of a GA, the system parameters were optimized in the study to determine their optimal settings for maximizing water production. The outcomes of this optimization process and their implications will be comprehensively discussed in the subsequent sections.

3.1. Results of statistical analysis of design variables in the WPS

Figure 2 presents the pairwise Pearson correlation coefficients between the design variables (AT, AH, AFR, and TL) and the water volume (WV) production of the condensation WPS. The analysis reveals a statistically significant correlation ($p < 0.01$) for all variable pairs, indicating a positive association between each design variable and WV production. In other words, increasing TL, AFR, AT, and AH results in a corresponding increase in system performance. Notably, AT, AH, TL, and AFR exhibit decreasing strengths of correlation with WV production, in that order.

Table 1 summarizes the ANOVA results for the factorial experiment evaluating the WPS's performance. These results demonstrate statistical significance of the main effects of all four design variables – AT, AH, AFR, and TL – on water volume (WV) production at the 1% level, except the TL–AFR interaction effect. Interestingly, the TL–AH interaction term exhibits statistically significant influence at the 5% level. These findings provide strong validation for the careful selection

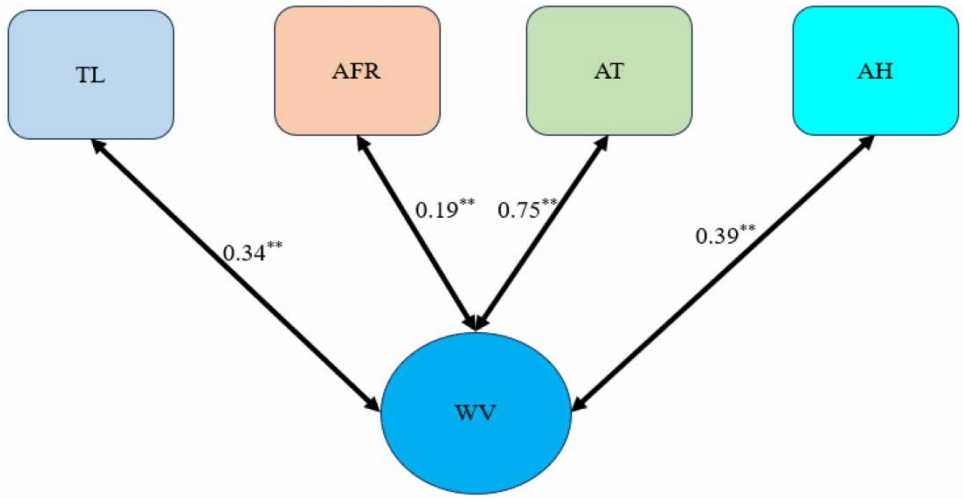

Figure 2 | Correlation analysis results between design variables and water production performance in the condensation WPS.

Table 1 | ANOVA results for design variables in the condensation WPS

Source of variation	DF	SS	MS	*f*-value	*p*-value
TL	1	915.56	915.56	1,482.69	0.00
AFR	2	270.79	135.40	219.27	0.00
AT	3	4,983.97	1,661.32	2,690.40	0.00
AH	3	1,192.30	397.43	643.62	0.00
TL × AFR	2	0.17	0.08	0.14	0.87
TL × AT	3	40.15	13.38	21.67	0.00
TL × AH	3	5.26	1.75	2.84	0.04
AFR × AT	6	67.79	11.30	18.30	0.00
AFR × AH	6	12.73	2.12	3.44	0.00
AT × AH	9	112.88	12.54	20.31	0.00
Error	249	153.76	0.62		
Total	287	7,755.35			

of TL, AFR, AT, and AH as key influencing factors and substantiate the effectiveness of the implemented experimental design and system configuration. Notably, this observation aligns with prior research findings in this area (Peeters *et al.* 2021).

Figure 3 visually dissects the relative contributions of the design variables (TL, AFR, AT, and AH) to water volume (WV) production within the condensation WPS. The data reveal distinct impact profiles for each variable on WV changes. Among these, AT emerges as the dominant factor, responsible for 64% of the variation, followed by AH (15%), TL (12%), and AFR (4%). These findings strongly resonate with the conclusions of Montazeri Saniji *et al.* (2023), highlighting the critical role of pipe burial depth, length, and volume in manipulating water extraction potential within condensation WPSs (Montazeri Saniji *et al.* 2023). Further supporting the significance of our chosen design variables, Peeters *et al.* (2021) emphasized the critical role of incoming AT, humidity, and speed as key determinants of water production in condensation WPSs. This reinforces the notion that manipulating these factors holds substantial potential for optimizing system performance (Peeters *et al.* 2021). The present study's findings provide further substantiation to these existing conclusions, emphasizing the critical role of optimizing AT, AH, TL, and AFR in enhancing the performance and efficiency of condensation WPSs. By optimizing these key variables, the potential for water extraction can be significantly improved, paving the way for more sustainable and effective water harvesting strategies.

3.2. Tuning of parameters for an SVM

The selection of the kernel function in SVM models is paramount, as it exerts a profound influence on the model's predictive accuracy. Each kernel function possesses unique characteristics, with some exhibiting a greater aptitude for capturing intricate patterns within the data. Figure 4 visually depicts the performance of various kernel functions within an SVM model for

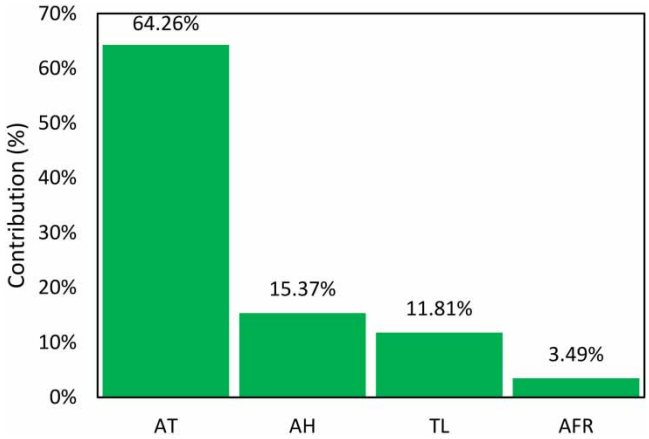

Figure 3 | Percentage of contribution of design variables on the performance of condensation WPS: AT, AH, AFR, and TL.

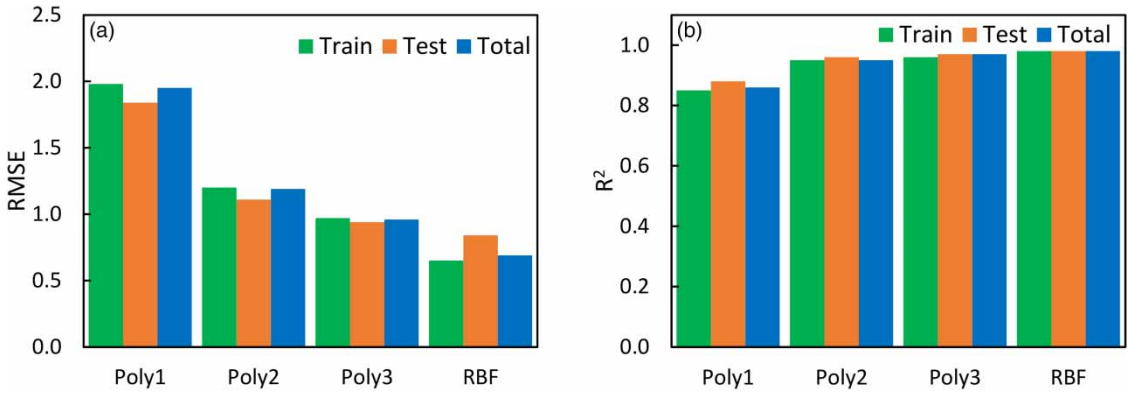

Figure 4 | Evaluation of kernel functions for optimal performance of the SVM model in water production performance: RMSE (a) and R^2 (b).

water production prediction, as assessed by RMSE (Figure 4(a)) and R^2 (Figure 4(b)) metrics. During model development, a comprehensive evaluation of different functions was conducted. Notably, the RBF, Poly3, Poly2, and Poly1 kernels demonstrated superior performance during the training, testing, and overall assessment stages, respectively. Ultimately, the RBF kernel emerged as the optimal choice for constructing the SVM model. This selection is rooted in the inherent complexity and nonlinear relationships between the input variables and water volume production within the system, which the RBF kernel effectively captures. By employing this kernel function, the SVM model adeptly uncovers intricate data patterns and facilitates precise predictions.

This study evaluated the efficacy of three solver algorithms (SMO, L1QP, and ISDA) for training and optimizing the hyperparameters of an LS-SVM model for predicting water volume production in condensation WPSs. Their performance was assessed using the RMSE (Figure 5(a)) and R^2 (Figure 5(b)) criteria across the training, testing, and overall datasets. As depicted in Figure 5, all three algorithms achieved strong correlations between predicted and actual values based on R^2 values, showing no significant differences. However, the RMSE metric revealed that ISDA did not outperform the other two. While SMO and L1QP exhibited comparable results in the training phase, L1QP demonstrated superior generalization performance in the testing phase, surpassing SMO. Consequently, L1QP was chosen for optimizing the LS-SVM model parameters. This algorithm minimizes a combined objective function consisting of a quadratic term and a linear term, while simultaneously enforcing sparsity on the weight vector through a constraint.

Within LS-SVM models, the box constraint parameter (C) serves as a pivotal factor in balancing model complexity and avoiding overfitting or underfitting. This parameter defines a hypercube in the Lagrange multiplier space, with its side length governed by C. By adjusting C, users influence the model's complexity: a larger value promotes a more complex model, while a smaller value leads to a simpler one. Selecting an appropriate C value is crucial to circumventing overfitting and underfitting. Figure 6 illustrates the evaluation of RMSE and R^2 changes in the SVM model for various C values, facilitating the identification of the optimal box constraint parameter for our study. The analysis revealed a box constraint value of

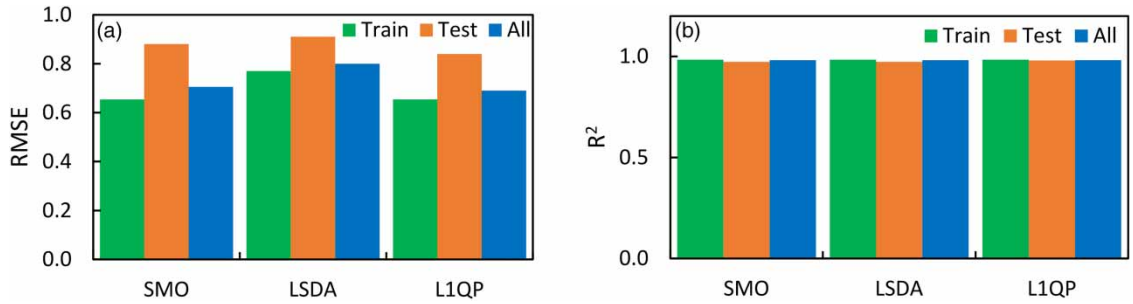

Figure 5 | Performance evaluation of the LS-SVM model with three solver algorithms (SMO, L1QP, and ISDA) for predicting water volume production in a condensation water production system: RMSE (a) and R^2 (b).

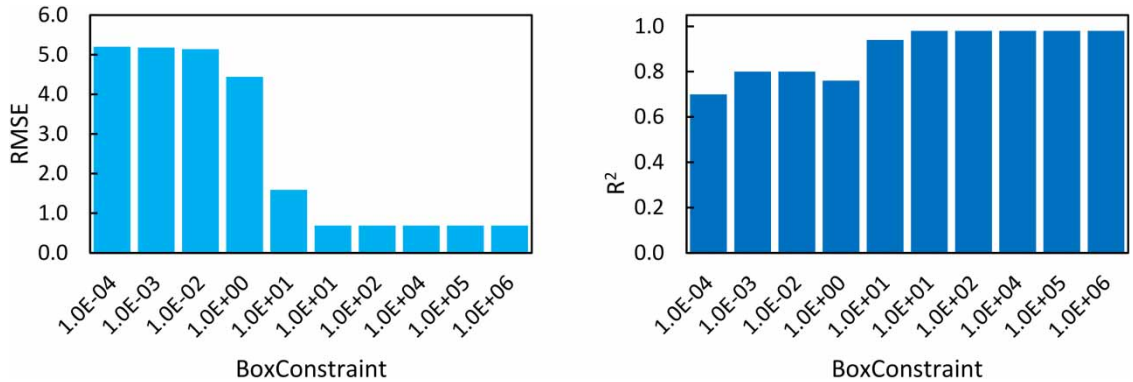

Figure 6 | Effect of box constraint parameter on the LS-SVM model performance for predicting water volume production in a condensation WPS.

10 as optimal, delivering both the minimum RMSE and the maximum R^2. Consequently, a C value of 10 was incorporated into the design of our SVM model for predicting water volume production in the condensation WPS.

3.3. A comprehensive study on the ability of SVM models to predict WPS performance

Following the optimization of the LS-SVM model's parameters and settings, the accuracy and reliability of its predicted water volume (WA) values were thoroughly assessed against the actual WV measurements. This evaluation provided valuable insights into the model's precision and consistency in WV prediction. In essence, the analysis aimed to validate the LS-SVM model's capability to predict WV for a condensation WPS by examining the agreement between its predictions and the actual data. As illustrated in Figure 7, the results reveal a remarkable performance by the SVM model, with a 98% agreement between the experimental data and the predicted values. Furthermore, the data points closely cluster around the 45 ° line, and the regression line parameters, exhibiting a slope near 1 and an intercept close to 0, further substantiate the model's accuracy. These findings collectively demonstrate the high effectiveness of the LS-SVM model in both WV prediction and modeling of the entire WPS, establishing it as a reliable tool with promising potential for future applications.

Generalizability assessment is critical for evaluating the performance of ML models, including LS-SVM, on unseen data. For predicting water volume (WA) production in a condensation WPS, gauging the model's ability to generalize to novel data is crucial to determine its real-world efficacy. Table 2 presents the results of such an assessment, where the training set size is varied from 50 to 90% to evaluate the SVM model's generalizability. Three performance metrics – RMSE, MAPE, and R^2 – are examined. The findings reveal an interesting trade-off: while reducing the training set size improves training performance, it can negatively impact testing performance. For instance, a 50% training set results in a testing phase prediction error of approximately 10.64%. However, a training set size of around 70% yields a lower error of 8%. In addition, an R^2 of 0.97 points to the SVM model's robustness in predicting WV, validating its prediction results. These findings offer valuable insights into the model's generalizability and its potential for practical applications.

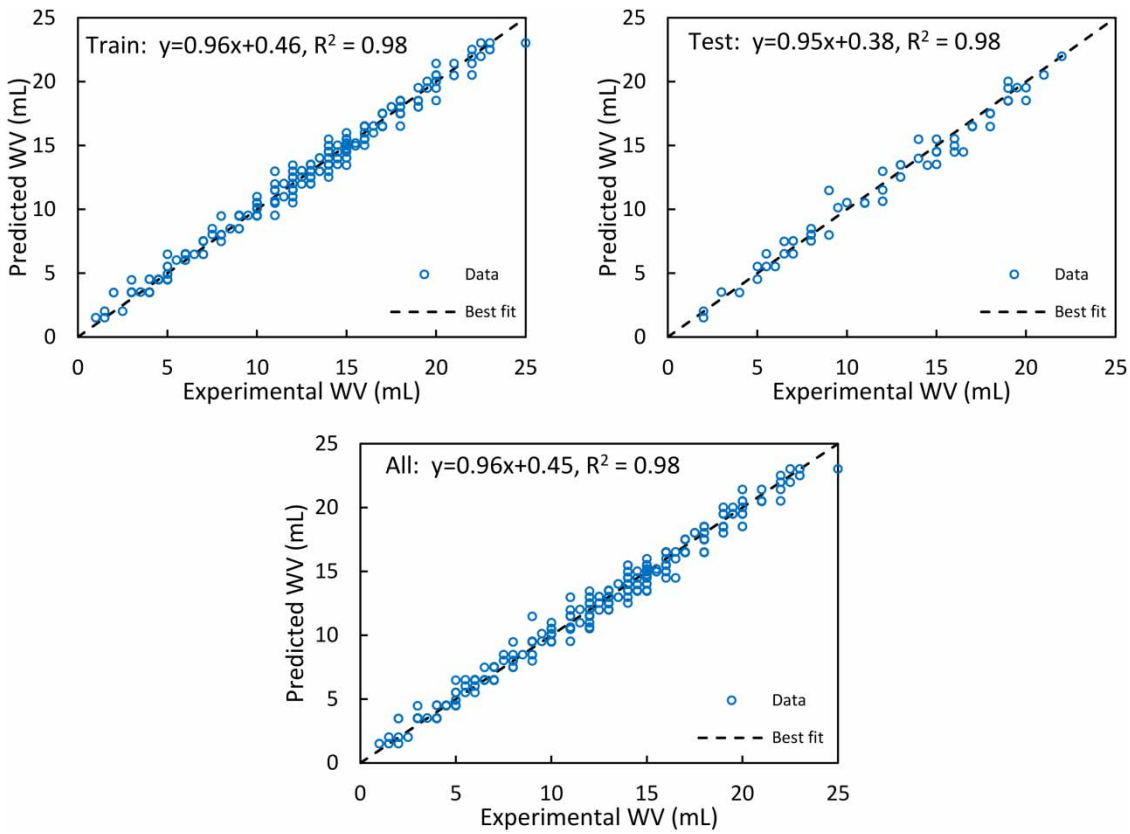

Figure 7 | Agreement analysis between experimental and predicted water volume production values in a condensation WPS using the LS-SVM model.

Table 2 | Generalizability evaluation of the SVM model for predicting water volume production in a condensation WPS

	Train			Test			All		
Training size (%)	RMSE	MAPE	R^2	RMSE	MAPE	R^2	RMSE	MAPE	R^2
90	0.65	6.02	0.98	0.67	4.18	0.98	0.66	5.99	0.98
80	0.65	6.02	0.98	0.84	6.52	0.98	0.69	6.12	0.98
70	0.58	5.48	0.99	0.98	7.77	0.97	0.72	6.16	0.98
60	0.59	5.43	0.99	1.17	10.88	0.96	0.86	7.61	0.98
50	0.54	5.53	0.99	1.32	10.64	0.94	1.01	8.09	0.96

3.4. Sensitivity analysis of independent variables for prediction of WPS performance using the LS-SVM model

Sensitivity analysis serves as a crucial tool for quantifying the individual influence of input variables on the prediction accuracy of ML models, including LS-SVM models for WPSs. In this context, such analysis can reveal the significance of independent variables – AT, AH, AFR, and TL – in predicting water volume (WV) production. By systematically removing each independent variable individually and evaluating its impact on model performance, we can identify the most critical variables contributing to system efficiency. This approach not only assists in prioritizing efforts for further optimization but also helps pinpoint potential sources of error and pave the way for model improvement.

Table 3 presents the results of the sensitivity analysis conducted on the SVM model with respect to the four input variables (AT, AH, TL, and AFR) across the training, testing, and overall stages. The findings reveal varying degrees of influence, ranging from significant to minimal, exerted by these variables on the model's prediction performance. Notably, removing AT from the input set yields the most substantial decline in R^2 and the most noticeable increases in RMSE and MAPE values. This translates to a roughly 2.5-fold decrease in model performance, underscoring the prominent role of AT in influencing system performance variations during WPS design.

3.5. Studying the performance of a WPS based on 3D response surface graphs

Response surface graphs provide a valuable tool for comprehending the intricate relationships between independent and dependent variables within a system. By visualizing data in three dimensions, these graphs facilitate the understanding of variable interactions and inform decision-making for system optimization toward maximum output based on input parameters. In our study, we utilized the results of the sensitivity analysis to generate 3D response surface graphs, offering valuable insights into the performance of a condensation WPS. Focusing on two key variables, AT and AH, plotted on the x and y axes, respectively, we gained deeper insights into their relationships with the dependent variable. To maintain scientific rigor, other variables were held at minimum, average, and maximum levels. The resulting six response surface graphs, three for TL at 2 m and three for TL at 4 m, with AFR values of 2.5, 5, and 7.5 m^3/h, facilitated the identification of optimal values for various input parameters. These graphs are illustrated in Figure 8(a)–8(f), enabling informed decision-making for system optimization and ultimately leading to a more efficient and effective WPS. An LS-SVM model was employed to generate the 3D response surface graphs. Figure 8 consistently demonstrates an increase in water volume (WV) as AT and AH values rise, regardless of AFR or TL. In addition, an upward trend in WV production is observed with increasing TL values. These consistent trends

Table 3 | Table sensitivity analysis results of the LS-SVM model for WPS performance prediction

	Train			Test			All		
	RMSE	MAPE	R^2	RMSE	MAPE	R^2	RMSE	MAPE	R^2
All	0.65	6.02	0.98	0.84	6.52	0.98	0.69	6.12	0.98
All excluding AFR	1.36	10.18	0.93	1.39	10.02	0.93	1.37	10.15	0.93
All excluding TL	1.97	17.63	0.85	2.75	23.94	0.74	2.15	18.90	0.83
All excluding AH	2.37	21.24	0.80	2.20	20.54	0.83	2.34	21.10	0.80
All excluding AT	4.43	53.15	0.33	5.23	60.91	0.16	4.60	54.72	0.30

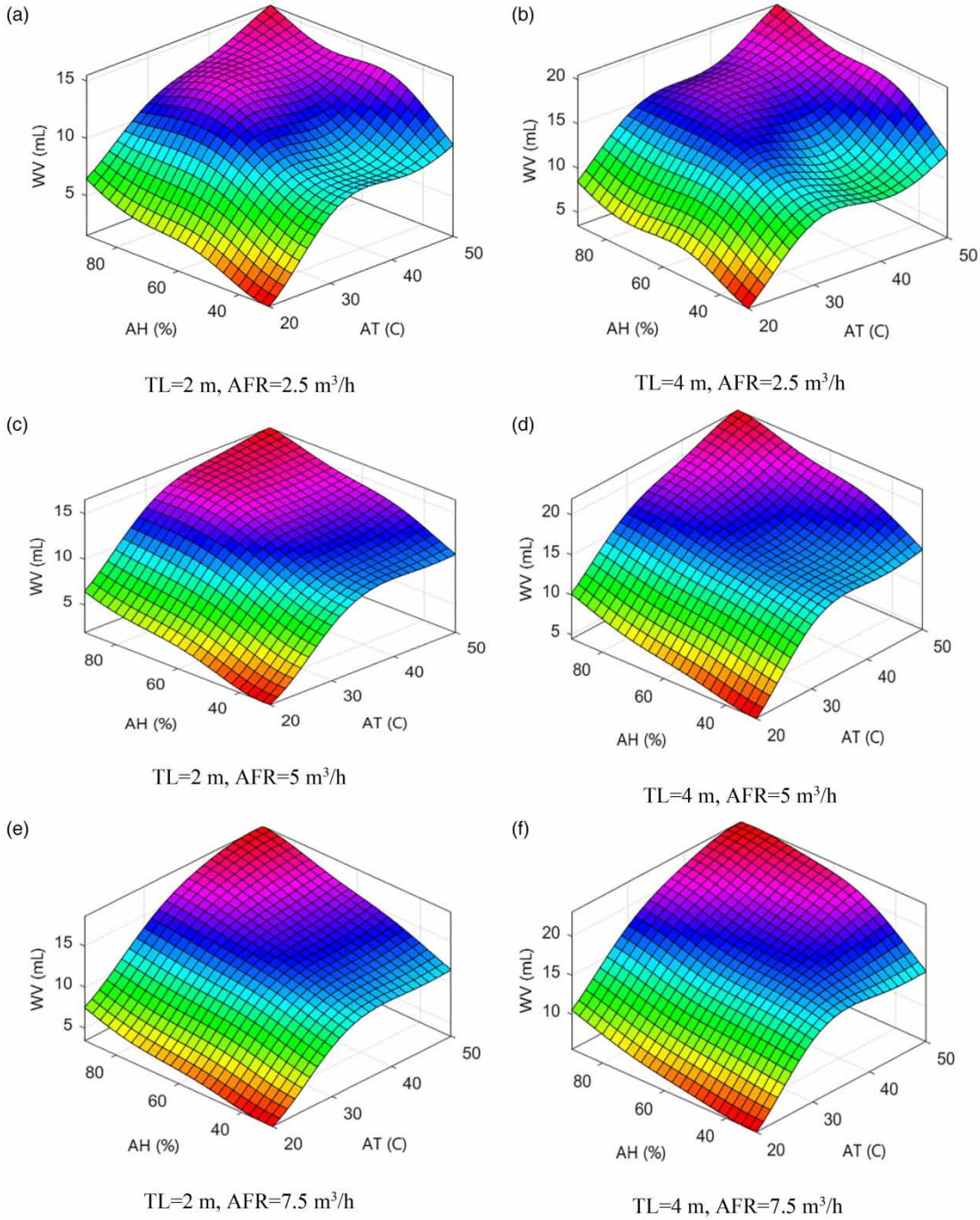

Figure 8 | 3D response surface graphs for the performance of a condensation WPS based on designed parameters (AT, AH, AFR, and TL).

across all cases affirm the mutual influences among the design variables within the system. The subsequent section will utilize the GA method to determine the optimal values for these variables.

3.6. Optimizing water production in a condensation WPS using a GA

To further enhance the efficiency of the condensation WPS, a GA was employed to identify the optimal values for its key parameters – TL, AFR, AT, and AH. The SVM model, previously validated for its accurate water volume (WA) estimations, served as the merit function within the GA optimization process. Following approximately 80 generations of feasible

solutions, the GA converged toward the optimal system configuration. This approach yielded optimal values of 3.98 m for TL, 6.89 m^3/h for AFR, 46.30 °C for AT, and 86.62% for AH, which led to a predicted WV production of 23.61 mL. Notably, the most effective treatment identified through experimental testing, utilizing a TL of 4 m, an AFR of 7.5 m^3/h, an AT of 50 °C, and an AH of 90%, resulted in a production of 23.50 mL. The close proximity of these values suggests that the solution proposed by the GA is near-optimal and likely to perform effectively in a real-world setting. However, further validation under larger-scale operational conditions may be warranted to definitively confirm the optimal performance of the WPS. Overall, the successful application of the GA demonstrates its potential for effectively optimizing the WPS, with the derived optimal values holding promise for enhancing system efficiency and performance.

Table 4 presents a comprehensive comparison of the performance characteristics and limitations of various water harvesting systems, providing valuable insights upon examination. The entries showcase a wide range of water production rates, from the modest 26 mL/h obtained by the thermoelectric cooler in the study by Eslami *et al.* (2018) to the impressive 1,200 L/day achieved by the solar-powered dew collector in the study by Yuan *et al.* (2011). This significant variability underscores the substantial influence of system selection on water extraction capabilities, with distinct capacities evident among different technologies. Solar-powered and multi-stage desiccant wheel systems emerge as robust contenders for large-scale water extraction, effectively meeting substantial and consistent water supply demands. The system of Tu & Hwang (2019), achieving an impressive rate of 32.5 kg/h, exemplifies this capability. In contrast, thermoelectric coolers and buried pipe condensation systems, often represented by the system of Elhammeli *et al.* (2017) producing 0.025 kg/s (0.091 m^3/h) of water, may find applications in specific microclimates or scenarios with modest water needs, offering more targeted or small-scale solutions. Environmental context and energy consumption play crucial roles in determining system performance. Systems like the thermoelectric cooler of Shourideh *et al.* (2018), achieving 1.584 L/day at 80% relative humidity (RH), exhibit sensitivity to specific humidity levels, while the soil–air water condensation system of Yao *et al.* (2021) relies on viable soil temperatures. In addition, energy efficiency considerations must be factored in. The thermoelectric cooler of Eslami *et al.* (2018) requires only 20 W for 26 mL of water production, contrasting significantly with the 550 W/m^2 average solar radiation needed for the dew collector of Yuan *et al.* (2011).

Our research contributes meaningfully to the diverse landscape of water harvesting technologies by exploring the potential of an air moisture–based system. Under optimal conditions, a promising water production rate of 23.61 mL/h is demonstrated by this system, expanding our understanding of this technology and its practical applications. While acknowledging its scale limitations, the viability of air moisture-based systems for specific needs or in conjunction with other approaches is underscored by our findings. The primary objective of this research is to develop a simple and cost-effective method for producing potable water from AH in low-capacity settings, particularly in remote and rural areas lacking access to reliable

Table 4 | Comparative analysis of recent studies on air moisture–based water harvesting approaches

WPS	Performance	Reference
Thermoelectric cooler	26 mL in 1 h at 318 K and 75% RH using 20 W	Eslami *et al.* (2018)
Multi-stage desiccant wheels	Water harvesting rate of 32.5 kg/h at 40 °C ambient temperature	Tu & Hwang (2019)
Thermoelectric cooler	1.584 L/day at 80% RH	Shourideh *et al.* (2018)
Condensation irrigation	Numerical simulations indicate 1.8 kg/m^2/day mean water production over 50 m pipe in a diurnally steady system	Lindblom & Nordell (2007)
Buried pipe condensation	Average water production of 0.025 kg/s (0.091 m^3/h) from humid air	Elhammeli *et al.* (2017)
Netting fog condensation water collector	Metal and polypropylene mesh collectors: average daily yields of 6.32 and 6.44 L/m^2, respectively	Kamali *et al.* (2022)
Soil–air water condensation system	Soil as a viable cold source for air condensation, extracting up to 2.2 kg of water in 20 h	Yao *et al.* (2021)
Solar-powered dew collector	Water production up to 1,200 L/day with average solar radiation of 550 W/m^2	Yuan *et al.* (2011)
Air moisture–based water harvesting system	23.61 mL/h under optimal conditions	This study

water sources. The system developed in this study can be employed in two distinct modes. First, solar energy can be harnessed in remote areas to provide the necessary electricity for controlling the room's environmental conditions. Second, in desert regions, moist air can be directed into a buried pipe without a control room and powered by wind energy, with the generated water used for drinking and agricultural purposes.

4. CONCLUSIONS

This study investigated the performance of a custom-designed WPS designed to extract water from AH across a range of operational parameters: AT, AH, AFR, and TL. Practical experiments established strong positive correlations between these variables and water production (WV). ANOVA further underscored the significance of the main and interactive effects of the variables, with the exception of TL × AFR at a 5% significance level.

To elucidate the complex relationships between these system variables, a meticulously developed LS-SVM model was implemented. Utilizing an RBF kernel function, a box constraint value of 10, and the L1QP algorithm, the LS-SVM model emerged as the optimal solution for the study. Its evaluation revealed an impressive 98% concordance between predicted and empirical data, with minimal errors of 0.66 mL and 5.99%.

Sensitivity analysis confirmed the varying roles of AT, AH, TL, and AFR in predicting system water production and overall performance, with their impact ranging from most to least influential, respectively. Subsequent application of a GA for optimization yielded optimal values of 3.98 m, 6.89 m^3/h, 46.30 °C, and 86.62% for TL, AFR, AT, and AH, respectively, leading to a substantial water production of 23.61 mL. Comparison with the best results from the experimental treatments further corroborated the validity of the optimization process.

While this research provides valuable insights into air moisture–based WPSs, it is crucial to acknowledge certain limitations that may influence the generalizability of its findings. The outcomes are inherently tied to the specific climatic and geographical conditions of the test area, potentially limiting direct applicability to diverse regions. In addition, the investigation of key variables assumes constant values for related factors, which might not fully capture the complexities of real-world scenarios. The focus on a limited range of variables and experiments emphasizes the need for cautious interpretation and motivates further research to validate and extend these initial findings.

To address these limitations, future research should consider repetitions in various geographical and weather conditions. A more comprehensive exploration of the system's functional variables, encompassing a broader range, is also recommended. Employing diverse variables in future studies, alongside advanced modeling and optimization methods, can bolster the reliability and generalizability of the system. This approach would ensure a more thorough evaluation of its production capabilities, ultimately contributing to the robustness and wider applicability of air moisture-based WPSs.

ACKNOWLEDGEMENTS

The authors gratefully acknowledge the support provided by the Vice Chancellor for Research and Technology of Shahid Chamran University of Ahvaz, Iran, under grant number 94/3/02/31579. We express our sincere appreciation to Shahid Chamran University of Ahvaz for their financial assistance, enabling the successful execution of this work. Special thanks are also extended to Mr Hosein Hoseinpour for his invaluable contribution in designing the 3D model of the system.

DATA AVAILABILITY STATEMENT

Data cannot be made publicly available; readers should contact the corresponding author for details.

CONFLICT OF INTEREST

The authors declare there is no conflict.

REFERENCES

Abraham, M. & Mohan, S. 2023 ANN-based PCA to predict evapotranspiration: A case study in India. *AQUA Water Infrastructure, Ecosystems and Society* **72** (7), 1145–1163.

Adnan, R. M., Mostafa, R. R., Dai, H.-L., Heddam, S., Kuriqi, A. & Kisi, O. 2023 Pan evaporation estimation by relevance vector machine tuned with new metaheuristic algorithms using limited climatic data. *Engineering Applications of Computational Fluid Mechanics* **17** (1), 2192258.

Alsirhani, A., Alshahrani, M. M., Abukwaik, A., Taloba, A. I., Abd El-Aziz, R. M. & Salem, M. 2023 A novel approach to predicting the stability of the smart grid utilizing MLP-ELM technique. *Alexandria Engineering Journal* **74**, 495–508.

Bergmair, D. 2015 *Design of A System for Humidity Harvesting Using Water Vapor Selective Membranes*. PhD thesis, Mechanical Engineering. Technische Universiteit Eindhoven, Netherlands.

Chen, L., Wu, T., Wang, Z., Lin, X. & Cai, Y. 2023 A novel hybrid BPNN model based on adaptive evolutionary Artificial Bee Colony Algorithm for water quality index prediction. *Ecological Indicators* **146**, 109882.

Elashmawy, M. & Alatawi, I. 2020 Atmospheric water harvesting from low-humid regions of Hail City in Saudi Arabia. *Natural Resources Research* **29**, 3689–3700.

Elhammeli, A. A., Muntasser, M. A., Lindblom, J. & Nordell, B. 2017 *Producing Water by Condensation of Humid Air in Buried Pipe*. IEOM Society, Rabat, Morocco, pp. 2270–2281.

Eslami, M., Tajeddini, F. & Etaati, N. 2018 Thermal analysis and optimization of a system for water harvesting from humid air using thermoelectric coolers. *Energy Conversion and Management* **174**, 417–429.

Essa, F., Elsheikh, A. H., Sathyamurthy, R., Manokar, A. M., Kandeal, A., Shanmugan, S., Kabeel, A., Sharshir, S. W., Panchal, H. & Younes, M. 2020 Extracting water content from the ambient air in a double-slope half-cylindrical basin solar still using silica gel under Egyptian conditions. *Sustainable Energy Technologies and Assessments* **39**, 100712.

Gerard, R. D. & Worzel, J. L. 1967 Condensation of atmospheric moisture from tropical maritime air masses as a freshwater resource. *Science* **157** (3794), 1300–1302.

Hajinajaf, S., Ghavami Jolandan, S. & Masoudi, H. 2021 Investigation of effective factors on water production system using land cooling. *Journal of Agricultural Engineering Soil Science and Agricultural Mechanization* **44** (3), 313–323.

Hanikel, N., Prévot, M. S., Fathieh, F., Kapustin, E. A., Lyu, H., Wang, H., Diercks, N. J., Glover, T. G. & Yaghi, O. M. 2019 Rapid cycling and exceptional yield in a metal-organic framework water harvester. *ACS Central Science* **5** (10), 1699–1706.

Hassan, A. A., Ezzeddine, M., Kordy, M. G. & Awad, M. M. 2023 *Atmospheric Water Harvesting Development and Challenges*. Springer, Cham, Switzerland, pp. 153–183.

He, H., Liu, L. & Zhu, X. 2022 Optimization of extreme learning machine model with biological heuristic algorithms to estimate daily reference evapotranspiration in Hetao Irrigation District of China. *Engineering Applications of Computational Fluid Mechanics* **16** (1), 1939–1956.

Kadhim, T. J., Abbas, A. K. & Kadhim, H. J. 2020 *Experimental Study of Atmospheric Water Collection Powered by Solar Energy Using the Peltier Effect*. IOP Publishing, Tomsk, Russia p. 012155.

Kamali, K., Nikkami, D., Abdoh Kolahchi, A., Pourghasem, A., Kazemi Dogholsar, H., Javadi Mojadad, D. & Davoodi, H. 2022 Water humidity collectors; New methods in alternative and sustainable water supply. *Water Harvesting Research* **5** (1), 53–66.

Kanooni, A. & Kohan, M. R. 2023 Fog water harvesting potential and its use in supplementary irrigation of rainfed crops (winter wheat) in Abi-beyglu, Ardabil (Iran). *Water Supply* **23** (9), 3675–3693.

Khalil, M. M., Kara-Ali, A. & Assad, M. 2022 Potential of harvesting water from fog and dew water over semi-arid and arid regions in Syria. *Water Supply* **22** (1), 874–882.

Koc, C., Koc, A., Gok, F. & Duran, H. 2020 Sustainable water harvesting from the atmosphere using solar-powered thermoelectric modules. *Polish Journal of Environmental Studies* **29** (2), 1197–1204.

LaPotin, A., Zhong, Y., Zhang, L., Zhao, L., Leroy, A., Kim, H., Rao, S. R. & Wang, E. N. 2021 Dual-stage atmospheric water harvesting device for scalable solar-driven water production. *Joule* **5** (1), 166–182.

Li, L., Shi, Z., Liang, H., Liu, J. & Qiao, Z. 2022 Machine learning-assisted computational screening of metal-organic frameworks for atmospheric water harvesting. *Nanomaterials* **12** (1), 159.

Lindblom, J. & Nordell, B. 2007 Underground condensation of humid air for drinking water production and subsurface irrigation. *Desalination* **203** (1–3), 417–434.

Liu, Y., Cao, Y., Wang, L., Chen, Z.-S. & Qin, Y. 2022 Prediction of the durability of high-performance concrete using an integrated RF-LSSVM model. *Construction and Building Materials* **356**, 129232.

Malik, A., Tikhamarine, Y., Al-Ansari, N., Shahid, S., Sekhon, H. S., Pal, R. K., Rai, P., Pandey, K., Singh, P. & Elbeltagi, A. 2021 Daily pan-evaporation estimation in different agro-climatic zones using novel hybrid support vector regression optimized by Salp swarm algorithm in conjunction with gamma test. *Engineering Applications of Computational Fluid Mechanics* **15** (1), 1075–1094.

Moazenzadeh, R., Mohammadi, B., Safari, M. J. S. & Chau, K.-w. 2022 Soil moisture estimation using novel bio-inspired soft computing approaches. *Engineering Applications of Computational Fluid Mechanics* **16** (1), 826–840.

Montazeri Saniji, M., Noori, S. & AzadManesh, A. 2023 Numerical simulation in atmospheric water generator by Ansys Fluent. *Journal of Renewable and New Energy* **10** (1), 32–45.

Peeters, R., Vanderschaeghe, H., Ronge, J. & Martens, J. A. 2021 Fresh water production from atmospheric air: Technology and innovation outlook. *Iscience* **24** (11), 1–21.

Shafeian, N., Ranjbar, A. & Gorji, T. B. 2022 Progress in atmospheric water generation systems: A review. *Renewable and Sustainable Energy Reviews* **161**, 112325.

Shourideh, A. H., Ajram, W. B., Al Lami, J., Haggag, S. & Mansouri, A. 2018 A comprehensive study of an atmospheric water generator using Peltier effect. *Thermal Science and Engineering Progress* **6**, 14–26.

Sleiti, A. K., Al-Khawaja, H., Al-Khawaja, H. & Al-Ali, M. 2021 Harvesting water from air using adsorption material – Prototype and experimental results. *Separation and Purification Technology* **257**, 117921.

Talib, A. J., Khalifa, A. H. N. & Mohammed, A. Q. 2019 Performance study of water harvesting unit working under Iraqi conditions. *International Journal of Air-Conditioning and Refrigeration* **27** (01), 1950011.

Tashtoush, B. & Alshoubaki, A. 2023 Atmospheric water harvesting: A review of techniques, performance, renewable energy solutions, and feasibility. *Energy* **280**, 128186.

Tu, R. & Hwang, Y. 2019 Performance analyses of a new system for water harvesting from moist air that combines multi-stage desiccant wheels and vapor compression cycles. *Energy Conversion and Management* **198**, 111811.

Tu, R. & Hwang, Y. 2020 Reviews of atmospheric water harvesting technologies. *Energy* **201**, 117630.

Tzanakakis, V. A., Paranychianakis, N. V. & Angelakis, A. N. 2020 *Water Supply and Water Scarcity*. MDPI, **12** (9), 2347.

Wahlgren, R. V. 2001 Atmospheric water vapour processor designs for potable water production: A review. *Water Research* **35** (1), 1–22.

Wang, W., Xie, S., Pan, Q., Dai, Y., Wang, R. & Ge, T. 2021 Air-cooled adsorption-based device for harvesting water from island air. *Renewable and Sustainable Energy Reviews* **141**, 110802.

Wang, Z., Wang, Q. & Wu, T. 2023 A novel hybrid model for water quality prediction based on VMD and IGOA optimized for LSTM. *Frontiers of Environmental Science & Engineering* **17** (7), 88.

Wu, J., Wang, Z., Hu, Y., Tao, S. & Dong, J. 2023 Runoff forecasting using convolutional neural networks and optimized bi-directional long short-term memory. *Water Resources Management* **37** (2), 937–953.

Yao, J., Wang, X., Zhu, J., Wang, B. & Niu, J. 2021 Experimental investigation of a novel extracting water system from air by soil cold source. *Mathematical Problems in Engineering* **2021**, 1–11.

Yuan, G., Wang, Z., Li, H. & Li, X. 2011 Experimental study of a solar desalination system based on humidification–dehumidification process. *Desalination* **277** (1–3), 92–98.

Zhang, G., Band, S. S., Ardabili, S., Chau, K.-W. & Mosavi, A. 2022 Integration of neural network and fuzzy logic decision making compared with bilayered neural network in the simulation of daily dew point temperature. *Engineering Applications of Computational Fluid Mechanics* **16** (1), 713–723.

Zhang, T., Xi, Y., Wang, H. & Zhang, Z. 2023a Surfaces with modified morphology and wettability arrangement: A potential medium for water harvesting in desertification areas. *Water Supply* **23** (8), 2972–2985.

Zhang, Z., Tang, H., Wang, M., Lyu, B., Jiang, Z. & Jiang, J. 2023b Metal–organic frameworks for water harvesting: Machine learning-based prediction and rapid screening. *ACS Sustainable Chemistry & Engineering* **11** (21), 8148–8160.

Zhou, J., Wang, D., Band, S. S., Mirzania, E. & Roshni, T. 2023 Atmosphere air temperature forecasting using the honey badger optimization algorithm: On the warmest and coldest areas of the world. *Engineering Applications of Computational Fluid Mechanics* **17** (1), 2174189.

First received 1 November 2023; accepted in revised form 12 February 2024. Available online 26 February 2024